UDC 621.396:621.391.82

A STATISTICAL MODEL OF INTERFERENCE IN WIRELESS NETWORKS, NETWORK-SCALE FADING AND OUTAGE PROBABILITY-NETWORK DENSITY TRADEOFF

V.I. MORDACHEV, S.L. LOYKA

Belarusian State University of Informatics and Radioelectronics
6, P. Brovki Str., Minsk, 220013, Belarus

School of Information Technology and Engineering, University of Ottawa
161 Louis Pasteur, Ottawa, Ontario, Canada, K1N 6N5

Submitted 23 February 2009

A novel statistical model of interference in wireless networks is proposed. The model is based on the traditional propagation channel model, which includes the average path loss as well as the large-scale and small-scale fading. In addition to these two traditional types of fading, a new concept of network-scale fading is introduced, which is due to a random spatial distribution of transmitters and receivers of the network over a large region of space occupied by the whole network. This new type of fading complements the small-scale (e.g. Rayleigh) and large-scale (e.g. log-normal) ones, is on the scale exceeding that of the other two and is independent of them. Its probability density function is derived for typical network configurations and propagation channel conditions. Network-level analysis of interference effects is given, which includes estimation of the average number of interferers, of the dynamic range of the interferers potentially capable of generating linear and non-linear distortion effects in the victim receiver, and of the outage probability. In many cases, the combined interference power at the receiver is shown to be dominated by the contribution of the strongest interferer. This analysis culminates in formulation of a tradeoff relationship between the network density and the outage probability. The positive role of linear filtering (e.g. in the antenna or in frequency filters of the receiver) in reducing the number and dynamic range of interfering signals, and/or in reducing the outage probability is quantified via a new statistical selectivity parameter (Q-parameter). The linear filtering allows increasing the network density by a factor of Q at the same outage probability.

Keywords: statistical model, interference, wireless networks, outage probability.

I. Introduction

Wireless communication networks have been recently a subject of extensive studies, both from information-theoretic and communication perspectives, including development of practical transmission strategies and fundamental limits (e.g. the network capacity scaling with the number of users) to assess the optimality of these strategies [1–6]. Multi-hop transmission has emerged as a promising mode of operation of ad-hoc wireless networks [2, 7–9], which has been shown to be order-optimal in certain scenarios [3–6].

From practical perspective, a performance of wireless networks (i.e. total throughput, error rates or outage probabilities, etc.) is limited, in one form or another, by mutual interference among several wireless links (e.g. several users) operating at the same time, so that some form of separation is required (i.e. in frequency, spatial location, etc.) [1, 2, 4, 7, 10, 11]. While some form of interference control (i.e. as in a multiple access scheme, by assigning different frequencies, time slots, codes, etc.) allows to decrease its effect on the network performance, it remains to be a bottleneck limiting the performance [10, 11]. Indeed, the ability of a receiver to eliminate interference created by unintended signals at its input (i.e. at the RF level, before IF and baseband processing) coming from all but the re-

quired user is limited due to a number of reasons, including imperfections of the hardware and the algorithms used [11, 12, 16]. For example, attenuation of out-of-band interferers is limited due to the limited performance of frequency filters and other functional blocks of the receiver; when interference power exceeds a certain threshold (e.g. 1 dB compression point, 3rd order intercept point (IP3), etc.), it also creates nonlinear distortions with the in-band frequency components (even if the interferers are out of band) at the RF level, which cannot be easily eliminated by IF or baseband processing [12]. Thus, careful analysis of interference effects is required during the network design stage to make sure that the receivers do not suffer from excessive distortions so that the link performance is at acceptable level, especially in the case of dense networks when a typical receiver is affected by a large number of interferers. Various types of the wireless channel fading should also be taken into account in such an analysis.

In this paper, we adopt this practical viewpoint and explore the effect of interference at the physical layer on the network performance. Specifically, we propose a statistical model of interference in a wireless network based on a model of random spatial distribution of the network transmitters, the standard propagation channel models, and the threshold-based model of the receiver performance (i.e. if the interference level does not exceed the threshold, the performance is satisfactory, if it does — the receiver as well as the link are considered to be in outage[1]).

The wireless propagation channel is known to have a significant effect on the link performance. In a typical analysis, the propagation path loss (or, equivalently, the received signal power) is separated into 3 independent factors, one deterministic and two random (fading): 1) the average path loss, 2) the large-scale fading (due to shadowing), and 3) the small-scale fading (due to multipath). The effects of these three factors on the link performance, including the interference effects, have been extensively studied [10, 11, 13–15]. In this paper, we demonstrate that, in the context of spatially-distributed wireless network with randomly-located nodes (i.e. transmitters and receivers), the first component, traditionally considered as deterministic (constant), also becomes random, due to random location of the nodes. This motivates us to introduce a concept of network-scale fading, which represents variations in the average received power coming from different randomly-located (but possibly fixed) transmitters. Clearly, this type of fading takes place on the network scale (see Fig. 1) and is complementary to the large-scale fading (i.e. shadowing) and small-scale fading (i.e. multipath), which take place on smaller scales.

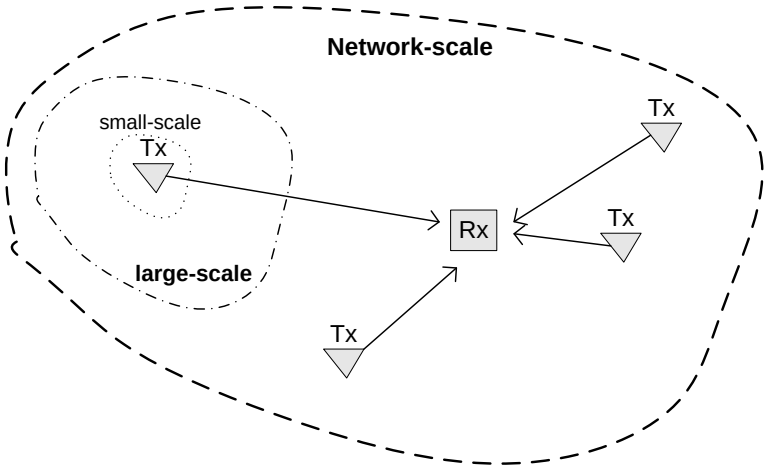

Fig. 1. Illustration of the problem geometry and three associated scales: small-scale (immediate neighborhood of a Tx; this is the scale of multipath fading), large-scale (extends beyond immediate neighborhood but is smaller than the whole network area; this is the scale of shadow fading) and network-scale (includes the whole network; this is the scale of network fading in (11)–(15)).

We derive the distribution function (of the average received power or the average channel gain) associated with the network-scale fading and, based on it, determine the outage probability of a given receiver (or, equivalently, of the link of a given user) when a number of randomly-located interferers (i.e. other users) are present. The total interference power

[1] While the traditional models of the receiver performance are based on the signal-to-interference plus noise ratio or on the signal-to-noise and interference-to-noise ratios [10, 11], our model is based on the interference power (or, equivalently, on the interference-to-noise ratio). The two are equivalent for the fixed required signal power. This is the case, for example, if the link has to perform satisfactory for a class of scenarios so that the design is based on the worst-case scenario, when the required signal power is at the minimum level (which corresponds, for example, to the required transmitter located at the cell boundary).

at the receiver input is shown to be dominated, in many cases, by the contribution of the strongest interferer so that its elimination (filtering out) can bring a significant gain. The case when a few most powerful interferers are eliminated in some way (e.g. by smart antennas, adaptive filtering etc.) is also considered. This analysis culminates in the formulation of the outage probability-network density tradeoff: for a given average density of the nodes, the outage probability is lower bounded or, equivalently, for a given outage probability, the average density of the nodes is upper bounded. This tradeoff is a result of the interplay between a random geometry of node locations, the propagation path loss and the distortion effects at the victim receiver. We also examine the positive effect of linear filtering at the receive end (by antennas, frequency filters, or any other type of linear processing) on this tradeoff via a new statistical filter gain. The analysis is based on the framework developed in [19–23].

The following are the main contributions of the paper: the concept of the network-scale fading and its distribution functions, the distribution of the interferers dynamic range (i.e. the maximum interference-to-noise ratio), the network density-outage probability tradeoff, and the impact of linear filtering on these performance measures via the statistical filter gain (Q-parameter).

The paper is organized as follows. Section II presents the system and network model, and basic assumptions. In Section III, we introduce the concept of network-scale fading and derive the distribution of received power and of the channel gain subject to this fading, for a single transmitter – receiver link. Section IV deals with the case of multiple, randomly-located interfering transmitters (users) affecting a victim receiver. The distribution of the dynamic range of interfering signals is derived. Based on this, Section V presets the outage probability — network density tradeoff. In Section VI, a positive effect of linear filtering on the outage probability — network density tradeoff is explored. Finally, Section VII concludes the paper.

II. Network and System Model

As an interference model of wireless network at the physical layer, we consider a number of point-like transmitters (Tx) and receivers (Rx) that are randomly located over a certain limited region of space S_m, which can be one ($m=1$), two ($m=2$),or three ($m=3$) -dimensional (1-D, 2-D or 3-D). This can model location of the nodes over a highway or a street canyon (1-D), a residential area (2-D), or a downtown area with a number of high-rise buildings (3-D). In our analysis, we consider a single receiver and a number of transmitters that generate interference to this receiver. We assume that the spatial distribution of the transmitters has the following properties:

For any two non-overlapping regions of space S_a and S_b, the probability of any number of Txs falling into S_a is independent of how many Txs fall into S_b, i.e. non-overlapping regions of space are statistically independent.

For infinitesimally small region of space dS, the probability $\mathrm{P}(k=1,dS)$ of a single transmitter ($k=1$) falling into dS is $\mathrm{P}(k=1,dS)=\rho dS$, where ρ is the average spatial density of transmitters (which can be a function of position). The probability of more than one transmitter falling into dS is negligible, $\mathrm{P}(k>1,dS)<<\mathrm{P}(k=1,dS)$ as $dS\to 0$.

Under these assumptions, the probability of exactly k transmitters falling into the region S is given by Poisson distribution [17, 18],

$$\mathrm{P}(k,S)=\frac{\bar{N}^k}{k!}e^{-\bar{N}} \tag{1}$$

where $\bar{N}=\int_S \rho dS$ is the average number of transmitters falling into the region S. If the density is constant, then $\bar{N}=\rho S$.

Possible scenarios to which the assumptions above apply, with a certain degree of approximation, are a sensor network with randomly-located non-cooperating sensors; a network(s) of mobile phones from the same or different providers (in the same area); a network of multi-standard wireless devices sharing the same resources (e.g. common or adjacent bands of frequencies).

Consider now a given transmitter-receiver pair. The power at the Rx antenna output P_r coming from the transmitter is given by the standard link budget equation [10, 11],

$$P_r = P_t G_t G_r g \tag{2}$$

where P_t is the Tx power, G_t, G_r are the Tx and Rx antenna gains, and g is the propagation path gain (=1/path loss),

$$g = g_a g_l g_s \tag{3}$$

where g_a is the average propagation path gain, and g_l, g_s are the contributions of large-scale (shadowing) and small-scale (multipath) fading. The widely-accepted model for g_a is [10, 11]

$$g_a = g_0 \left(R_0 / R \right)^{\nu} = a_\nu R^{-\nu} \tag{4}$$

where ν is the path loss exponent, R_0 is the reference distance, g_0 is the average path gain at this distance, and $a_\nu = g_0 R_0^{\nu}$. Typical values of ν are as follows: for free space, $\nu = 2$; for two-ray propagation model (with line-of-sight and ground reflection at low elevation angle), $\nu = 4$; for typical urban macrocellular environment, $\nu = 3...4$; for microcellular environment, $\nu = 2...8$ [11]. Extensive measurement campaigns have been undertaken to characterize ν more accurately in various environments [10].

When the Tx and Rx antennas are isotropic, $G_t = G_r = 1$, and the power at the Rx input is

$$P_{is} = P_r \big|_{G_t = G_r = 1} = \frac{c_\nu P_t}{R^{\nu}} g_l g_s \tag{5}$$

where c_ν absorbs the effects of ν, g_0, R_0 that are independent of R, P_t, g_l, g_s. Thus, (2) and (5) can be used to evaluate the signal power at the Rx input coming from each transmitter.

III. Distribution of Average Path Loss and Average Power at the Receiver

In this section, we consider a single randomly-located interfering transmitter and a fixed position victim receiver. The statistics of the isotropic Rx power P_{is} coming from this transmitter depends on the distribution of $g = g_a g_l g_s$ and thus on the joint distribution of g_a, g_l, g_s. The last two factors can be modeled as independent log-normal and Rayleigh (Rice) distribution, respectively [10, 11]. Contrary to the traditional approach to the analysis of point-to-point systems, g_a in our network-level model is also a random variable, since the Tx-Rx distance R in (4) is random (due to random location of the transmitter) and it is this random variable that represents the network-scale fading. Since g_a in (4) does not depend on the local propagation environment around the Tx or Rx ends that affect g_l, g_s but only on the global configuration of the Tx-Rx propagation path (including the distance R, of which g_l, g_s are independent) [10, 11], g_a in this model is independent of g_l, g_s, which is ultimately due to different physical mechanisms responsible for g_a, g_l, g_s. Thus, the join probability density function (PDF) of g_a, g_l, g_s is

$$f(g_a, g_l, g_s) = f_a(g_a) f_l(g_l) f_s(g_s) \tag{6}$$

where $f_a(g_a), f_l(g_l), f_s(g_s)$ are the PDFs of g_a, g_l, g_s, respectively. The PDF of g can be found from

$$f_g(x) = \iint f_a(g_a) f_l(g_l) f_s\left(\frac{x}{g_a g_l} \right) dg_a dg_l \tag{7}$$

The effects of small-scale and large-scale fading on the link performance, including the interference effects, have been extensively analyzed in the past [10, 11, 13–15]. Thus, we concentrate on the network-scale fading and its effects by assuming $g_l = g_s = 1$ (equivalently, we consider the path gain averaged over large and small-scale fading), and leave the study of combined effects of all three types of fading for future research.

Using (4), it is straightforward to find $f_a(g_a)$ for given PDF $f_R(R)$ of the Tx-Rx distance,

$$f_a(g_a) = f_R(R)\left|dg_a / dR\right|^{-1} \tag{8}$$

To find the PDF $f_R(R)$ of the Tx-Rx distance, we consider a fixed-position receiver (e.g. a base station) and a randomly-positioned transmitter (e.g. a mobile unit). Using the PDF of the Tx position $f_t(\mathbf{x})$ in the Cartesian reference frame, where $\mathbf{x}$ is the Tx position vector, $\mathbf{x} = [x, y, z]^T$ if $m = 3$, $\mathbf{x} = [x, y]^T$ if $m = 2$, and $\mathbf{x} = x$ if $m = 1$, one obtains the corresponding PDF in the spherical reference frame,

$$f_t(r, \theta, \varphi) = f_t(\mathbf{x})\left|\frac{\partial(x, y, z)}{\partial(r, \theta, \varphi)}\right| = f_t(\mathbf{x}) \cdot r^2 \cos\theta d\theta d\varphi dr, \ m = 3 \tag{9}$$

$$f_t(r, \varphi) = f_t(\mathbf{x})\left|\frac{\partial(x, y)}{\partial(r, \varphi)}\right| = f_t(\mathbf{x}) \cdot r dr d\varphi, \ m = 2$$

where $r \geq 0$ is the radius, $0 \leq \varphi \leq 2\pi$ is the azimuth, $-\pi/2 \leq \theta \leq \pi/2$ is the elevation angle; $\left|\partial(x, y, z)/\partial(r, \theta, \varphi)\right|$ and $\left|\partial(x, y)/\partial(r, \varphi)\right|$ are the Jacobians of the transformation; $x = r\cos\theta\cos\varphi$, $y = r\cos\theta\sin\varphi$, $z = r\sin\theta$ for $m = 3$, and $x = r\cos\varphi$, $y = r\sin\varphi$ for $m = 2$. Assuming that the receiver is positioned at $\mathbf{x} = \mathbf{0}$ (the origin), the PDF of the Tx-Rx distance can be obtained by integrating $f_t(r, \theta, \varphi)$ and $f_t(r, \varphi)$ over (θ, φ) and φ, respectively, and can be expressed as

$$f_R(R) = R^{m-1} f_m(R) \tag{10}$$

where

$$f_3(R) = \int_0^{2\pi}\int_{-\pi/2}^{\pi/2} f_t(\mathbf{x})\cos\theta d\theta d\varphi, \ f_2(R) = \int_0^{2\pi} f_t(\mathbf{x}) d\varphi,$$
$$f_1(R) = f_t(R) + f_t(-R)$$

and the integrals are over $|\mathbf{x}| = R$.

We consider below the PDF in (10) over a limited range of R, $R_{\min} \leq R \leq R_{\max}$, where the minimum distance $R_{\min}$ is due to the geometrical, design or regulatory constrains (e.g. a minimum possible distance between a base station and a mobile unit), and the maximum distance $R_{\max}$ is such that the signal power at the Rx input coming from the transmitter located at that distance, which corresponds to the minimum path gain $g_{\min} = g_a(R_{\max})$, is equal to the noise power P_0 at the receiver, $P_0 = P_t g_{\min} \rightarrow R_{\max} = (a_v P_t / P_0)^{1/v}$. All received signals of lower power, i.e. the signals that are below the Rx noise level[2], are ignored in our analysis. Thus, only the transmitters located in the potential interference zone (see Fig. 2) are taken into account. Finally, the PDF $f_a(x)$ of g_a is

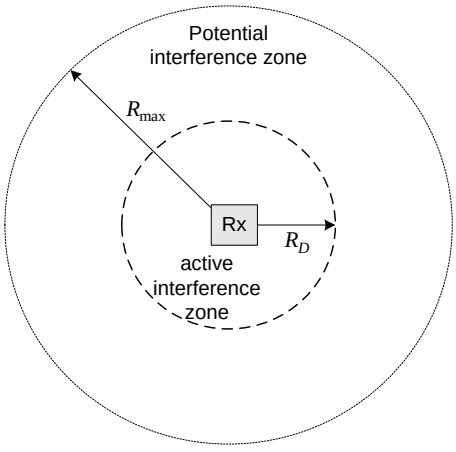

Fig. 2. Interference zones on the network scale. Potential interference zone: $R \leq R_{\max}$, $P_a(R) \geq P_0 = P_a(R_{\max})$ (the signal power exceeds the Rx noise level); active interference zone: $R \leq R_D$, $P_a(R) \geq P_{df} = R_a(R_D)$ (the signal power exceeds the maximum distortion-free power)

[2] Minimum detectable signal level [12] can also be considered instead of the noise level.

$$f_a(x) = \frac{a_\nu^m}{\nu} \frac{f_m((a_\nu / x)^{1/\nu})}{x^{1+m/\nu}} \tag{11}$$

Corresponding CDF can be obtained by integration.

In the case of the uniform spatial PDF of transmitter location, $f_t(\mathbf{x}) = \text{const}$, (11) takes a simple form,

$$f_a(x) = \frac{b_{\nu m}}{x^{1+m/\nu}},\ b_{\nu m} = \frac{m}{\nu} \left(g_{\min}^{-m/\nu} - g_{\max}^{-m/\nu} \right)^{-1},\ g_{\min} \le x \le g_{\max} \tag{12}$$

$$F_a(x) = \left(g_{\min}^{-m/\nu} - g_{\max}^{-m/\nu} \right)^{-1} \left(g_{\min}^{-m/\nu} - x^{-m/\nu} \right),$$

where $g_{\min} = g_a(R_{\max}) = P_0 / P_t$, $g_{\max} = g_a(R_{\min}) = a_\nu R_{\min}^\nu \le 1$[3], and $F_a(x)$ is the CDF of g_a. In many cases of practical interest, $g_{\max}$ significantly exceeds $g_{\min}$, $g_{\min} << g_{\max}$ (e.g. $g_{\min} \approx 10^{-10}...10^{-15}$ and $g_{\max} \approx 10^{-3}...1$). In such a case, the upper bound can be eliminated without significant loss in accuracy[4] and (12) simplifies to

$$f_a(x) = \frac{m g_{\min}^{m/\nu}}{\nu x^{1+m/\nu}},\ F_a(x) = 1 - \left(\frac{g_{\min}}{x} \right)^{m/\nu},\ x \ge g_{\min} \tag{13}$$

In a similar way, one can find the distribution of the average isotropic power $P_a = P_t g_a$ at the receiver. In fact, (12), (13) apply with the substitution $P_a \to g_a$, $P_{1(0)} \to g_{\min(\max)}$,

$$w_a(x) = \frac{1}{P_t} f_a(g)\big|_{g = x/P_t} = f_a(g)\big|_{x \to g,\, P_{1(0)} \to g_{\min(\max)}} \tag{14}$$

$$W_a(x) = F_a(x / P_t) = \left(P_0^{-m/\nu} - P_1^{-m/\nu} \right)^{-1} \left(P_0^{-m/\nu} - x^{-m/\nu} \right)$$

where $w_a(x)$ and $W_a(x)$ are the PDF and CDF of P_a, respectively, and $P_1 = P_t g_{\max}$ is the maximum power. In the case when the Tx and Rx antenna patters do not affect the statistics considered above, the same applies to the Rx power with non-isotropic antennas $P_r = P_t G_t G_r g_a$. When $P_1 / P_0 >> 1$, (14) simplifies to

$$w_a(x) = \frac{m P_0^{m/\nu}}{\nu x^{1+m/\nu}},\ W_a(x) = 1 - \left(\frac{P_0}{x} \right)^{m/\nu},\ x \ge P_0 \tag{15}$$

which is an equivalent of (13). The probability that the interference power exceeds level $x \ge P_0$, which is the complementary cumulative distribution function (CCDF) of P_a, can be simply expressed as

$$\Pr\ P_a > x = 1 - W_a(x) = \left(P_0 / x \right)^{m/\nu},\ x \ge P_0 \tag{16}$$

Fig. 3 shows this probability evaluated via Monte-Carlo simulations and via (16). Note good agreement between the two, which also validates the approximation in (15), (16). Comparison of the $\nu = 2$ and $\nu = 4$ cases shows that, for given threshold level P_a / P_0 (e.g. 40 dB), this probability is significantly larger for the latter (10^{-2} vs. 10^{-4} for the former).

[3] The last constraint is due to the fact that the Rx power cannot exceed the Tx power.

[4] This is similar to the log-normal and Rayleigh (Rice) distributions, which have no upper bound and thus can formally violate the law $P_r \le P_t$, but this does not affect significantly the accuracy of the analysis.

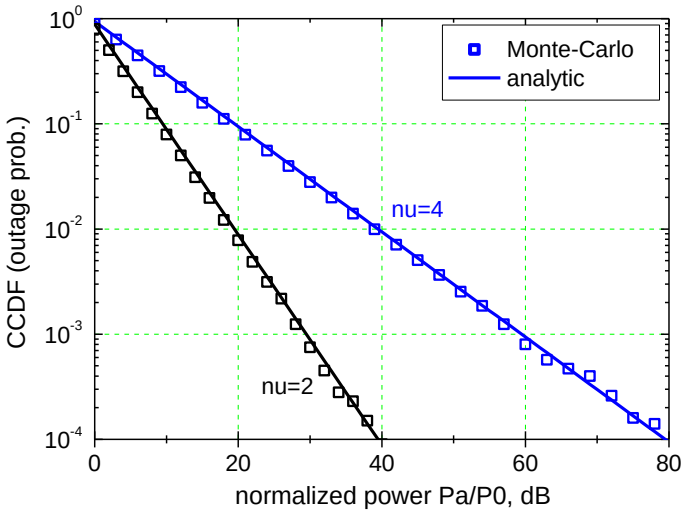

Fig. 3. The CCDF of P_a/P_0 evaluated from Monte-Carlo (MC) simulations (10^5 trials) and from (15) for m=2, ν=2&4

Alternatively, for given outage probability (e.g. 10^{-3}), the threshold level P_a / P_0 (i.e. "outage interference power") for the $\nu = 4$ case significantly exceeds that of the $\nu = 2$ case (60 dB vs. 30 dB). This is explained by the fact that, when the transmitter moves closer to the receiver, the signal power grows much faster for the $\nu = 4$ case (two-ray propagation), which, combined with the uniform PDF of the transmitter location, gives the observed result.

It should also be pointed out that (15), (16) holds also under more general assumptions as long as $P_1 / P_0 >> 1$ holds [19, 21, 22]: (i) for transmitters with different powers P_{ti} (note that (15), (16) are independent of P_t), (ii) for the uniform spatial distribution of transmitters on the spherical earth and the receiver elevated over the earth (i.e. a base station antenna), and (iii) when linear filtering (over angles of arrival, frequency, polarization etc.) is used.

Based on (12) and (14), one can find the mean value of P_a,

$$\bar{P}_a = \int_{P_0}^{P_1} x w_a(x) dx = \begin{cases} \dfrac{P_0 D_1^{1-m/\nu} \;\; 1 - D_1^{m/\nu - 1}}{\nu/m - 1 \;\; 1 - D_1^{-m/\nu}}, & m \neq \nu \\ \dfrac{P_0}{1 - D_1^{-1}} \ln \;\; D_1 \;\;, & m = \nu \end{cases} \tag{17}$$

where $D_1 = P_1 / P_0$. In the important case of $D_1 = P_1 / P_0 >> 1$, (17) simplifies to

$$\bar{P}_a \approx \begin{cases} \dfrac{P_0 D_1^{1-m/\nu}}{\nu/m - 1}, & m < \nu \\ P_0 \ln \;\; D_1 \;\;, & m = \nu \\ \dfrac{P_0}{1 - \nu/m}, & m > \nu \end{cases} \tag{18}$$

To gain some insight, let us consider two special cases: (i) $m = \nu = 2$ (flat earth distribution and free-space (i.e. dominant line-of-sight) propagation), and (ii) $m = 2, \nu = 4$ (i.e. two-ray (ground reflection) propagation and flat-earth distribution),

$$\bar{P}_a \approx P_0 \ln \;\; D_1 \;\;, \; m = \nu = 2 \,; \; \bar{P}_a \approx P_0 \sqrt{D_1} \;, \; \nu / m = 2 \tag{19}$$

In both cases, $\bar{P}_a$ is a slowly increasing function of D_1, and $\bar{P}_a << P_1$, i.e. the mean value $\bar{P}_a$ cannot be used to estimate adequately the harmful effect of high-power interferers ($>> \bar{P}_a$), which appear with non-vanishing probability and may cause severe linear and nonlinear (e.g. intermodulation, harmonics, noise conversion etc.) distortions in the receiver, even if the interferers are out-of-band.

To overcome this difficulty, we introduce and analyze in the next section the dynamic range of interferers, which adequately represents the possibility of interference effects in the receiver due to high-power ($>> \bar{P}_a$) interferers.

IV. Dynamic Range of Interfering Signals

In this section, we consider a fixed-position receiver (e.g. a base station of a given user) and a number of randomly located interfering transmitters (interferers, e.g. mobile units of other users) of the same power P_t. As in the previous section, we consider only the network-scale fading, assuming $g_l = g_s = 1$ (i.e. we consider the Rx signal power averaged over large- and small-scale fading). We assume that the Rx antenna is isotropic and consider the signals at the Rx input. The impact of linear filtering (e.g. by antennas, frequency filters of the receiver, etc.) is considered in section VI.

The statistics of transmitters' location is given by (1). Transmitter *i* produces the average power $P_{ai} = P_t L_a(R_i)$ at the receiver input, and we consider only the signals exceeding the Rx noise level $P_{ai} \geq P_0$. The dynamic range in the ensemble of the interfering signals is defined via the most powerful (at the Rx input) signal,

$$d_a = P_{a1} / P_0 \tag{20}$$

where, without loss of generality, we index the transmitters in the order of decreasing Rx power, $P_{a1} \geq P_{a2} \geq ... \geq P_{aN}$. Equivalently, d_a is the largest interference-to-noise ratio (INR). The most powerful signal is coming from the transmitter located at the minimum distance r_1, $P_{a1} = P_t g_a(r_1)$. The statistics of the minimum distance can be found from the observation that the sphere $V(r_1)$ of radius r_1 contains no transmitters and the spherical shell $\Delta V(r_1, r_1 + \Delta r)$ of radii $r_1, r_1 + \Delta r$ contains exactly one transmitter, as $\Delta r \to 0$ [19, 20, 22]. The probability of this event is

$$p(1, \Delta V)\, p(0, V) = \bar{N}(\Delta V) e^{-\bar{N}(V)} = f_r(r_1)\Delta r \tag{21}$$

where $\bar{N}(\Delta V) = \int_{\Delta V} \rho dV = \bar{N}(V(r_1 + \Delta r)) - \bar{N}(V(r_1))$ and $\bar{N}(V) = \int_V \rho dV$ are the average number of transmitters in ΔV and V, respectively, and $f_1(r)$ is the PDF of r_1. Using (21), one obtains

$$f_1(r) = -\frac{de^{-\bar{N}}}{dr} = \frac{d\bar{N}}{dr} e^{-\bar{N}} = e^{-\bar{N}} \int_{V'(r)} \rho dV \tag{22}$$

where $\bar{N} = \bar{N}(V(r))$ is the average number of transmitters in the ball $V(r)$, $V'(r)$ is sphere of radius r and the integral in (22) is over this sphere. The cumulative distribution function (CDF) of r_1 is

$$F_1(r) = 1 - e^{-\bar{N}} \tag{23}$$

The probability that the dynamic range exceeds value D is $\Pr\ d_a > D\ = \Pr\ r_1 < r(D)\ = F_1(r(D))$, where $r(D)$ is such that $P_a(r(D)) = P_0 D$, so that the CDF of d_a is

$$F_d(D) = 1 - \Pr\ d_a > D\ = e^{-\bar{N}} = \exp\ -\int_{V\ r(D)} \rho dV\ ,\ r(D) = \left(\frac{P_t a_\nu}{P_0 D} \right)^{\frac{1}{\nu}} \tag{24}$$

where $\bar{N}$ is the average number of transmitters in the ball $V\ r(D)$ of radius $r(D)$. The corresponding PDF can be obtained by differentiation,

$$f_d(D) = \frac{r(D) e^{-\bar{N}}}{\nu D} \int_{V'(r(D))} \rho dV \tag{25}$$

When the average spatial density of transmitters is constant, $\rho = const$, (24), (25) simplify to

$$F_d(D) = \exp\left\{ -c_m \rho \left(\frac{P_t a_\nu}{P_0 D} \right)^{m/\nu} \right\} = \exp\ -\bar{N}_{\max} D^{-m/\nu}\ ,\ f_d(D) = \frac{m}{\nu} \bar{N}_{\max} D^{-m/\nu - 1} \exp\ -\bar{N}_{\max} D^{-m/\nu} \tag{26}$$

where $\overline{N}_{\max} = c_m R_{\max}^m \rho$ is the average number of transmitters in the potential interference zone (see Fig. 2), $c_1 = 2$, $c_2 = \pi$ and $c_3 = 4\pi/3$.

When $(k-1)$ most powerful signals, which are coming from $(k-1)$ closest transmitters, do not create any interference (i.e. due to frequency, time or code separation in the multiple access scheme, or due to any other form of separation or filtering), the CDF and PDF of the distance r_k to the most powerful interfering signal of order k is [19, 22]

$$F_k(r) = 1 - e^{-\bar{N}} \sum_{i=0}^{k-1} \frac{\bar{N}^i}{i!}, \quad f_k(r) = \frac{dF_k(r)}{dr} = \frac{\bar{N}^{k-1} e^{-\bar{N}}}{(k-1)!} \int_{V'(r)} \rho dV \tag{27}$$

where $\bar{N} = \int_{V\ r} \rho dV$ is, as above, the average number of signals in $V\ r$. The CDF of the dynamic range d_a is given by (27) evaluated at $r = r(D) = \left(\frac{P_t a_\nu}{P_0 D} \right)^{1/\nu}$,

$$F_{dk}(D) = e^{-\bar{N}} \sum_{i=0}^{k-1} \frac{\bar{N}^i}{i!} = F_k \left(\left(\frac{P_t a_\nu}{P_0 D} \right)^{1/\nu} \right) \tag{28}$$

where $\bar{N} = \bar{N}\ V\ r\ D$ is the average number of signals in $V\ r\ D$. In the case of constant average density $\rho = const$, the CDF and PDF of d_a simplify to

$$F_{dk}(D) = \exp\ -\overline{N}_{\max} D^{-m/\nu}\ \sum_{i=0}^{k-1} \frac{1}{i!} \left(\frac{\overline{N}_{\max}}{D^{m/\nu}} \right)^i, \quad f_{dk}(D) = \frac{m}{\nu} \frac{\overline{N}_{\max}^k}{(k-1)!} D^{-\frac{km}{\nu}-1} \exp\ -\overline{N}_{\max} D^{-m/\nu} \tag{29}$$

The mean minimum distance $\overline{r}_1$ can be evaluated from (29) as follows [19, 20, 22]

$$\overline{r}_1 = \frac{\Gamma(k + 1/m)}{\Gamma(k)\ c_m \rho^{\ 1/m}} \tag{30}$$

where Γ is the gamma function.

V. Outage Probability-Network Density Tradeoff

Powerful interfering signals can result in significant performance degradation due to linear and nonlinear distortion effects in the receiver when they exceed certain limit (e.g. maximum tolerable INR, 1dB compression point, 3rd order intercept point etc.), which we characterize here via the receiver distortion-free dynamic range $D_{df} = P_{\max} / P_0$, where $P_{\max}$ is the maximum interfering signal power at the receiver that does not cause significant performance degradation [12]. If $d_a > D_{df}$, there is significant performance degradation and the receiver is considered to be in outage[5], which corresponds to one or more transmitters falling into the active interference zone (see Fig. 2), whose probability is

$$\mathrm{P}_{out} = \Pr\ d_a > D_{df}\ = 1 - F_d(D_{df}) \tag{31}$$

For given P_{out}, one can find the required distortion-free dynamic range ("outage dynamic range") D_{df}

$$D_{df} = F_d^{-1}(1 - \mathrm{P}_{out}) \tag{32}$$

[5] In our analysis, outage is linked to the interfering signal power exceeding a certain threshold, rather than to the required signal power dropping below a certain threshold, which is typically the case in the literature.

We note that, in general, D_{df} is a decreasing function of P_{out}, i.e. low outage probability calls for high distortion-free dynamic range. For simplicity of notations, we further drop the subscript and denote the spurious-free dynamic range by D.

A. All interfering signals are active (*k*=1)

We consider first the case of $k=1$, i.e. all interfering signals are active. The outage probability can be evaluated using (24) and (31). From practical perspective, we are interested in the range of small outage probabilities $\mathrm{P}_{out} << 1$, i.e. high-reliability communications. When this is the case, $F_d(D) \to 1$ and using MacLaurean series expansion $e^{-\bar{N}} \approx 1 - \bar{N}$, (31) simplifes to

$$\mathrm{P}_{out} \approx \overline{N} = \int_{V\ r(D)} \rho dV \tag{33}$$

which further simplifies, in the case of $\rho = const$, to

$$\mathrm{P}_{out} \approx \overline{N}_{\max} D^{-m/\nu} \tag{34}$$

Note that, in this case, the outage probability P_{out} scales linearly with the average number $\overline{N}_{\max}$ of nodes in the potential interference zone, and it effectively behaves as if the number of nodes were fixed (not random) and equal to $\overline{N}_{\max}$. In the case of $\overline{N}_{\max} = 1$, (34) reduces to (16) (i.e. to the case of a single interfering transmitter). Based on these two observations, we conclude that the single-order events (i.e. when only one signal in the ensemble exceeds the threshold) are dominant contributor to the outage. This immediately suggests a way to reduce significantly the outage probability by eliminating (e.g. by filtering) the dominant interferer in the ensemble. Using (34), the required spurious-free dynamic range of the receiver can be found for given outage probability,

$$D \approx \left. \overline{N}_{\max} \right/\!\!/ \mathrm{P}_{out}^{\ \nu/m} \tag{35}$$

Note that higher values of ν and lower values for m call for higher dynamic range. Intuitively, this can be explained by the fact that when the transmitter moves from the boundary of the potential interference zone (i.e. $R = R_{\max}$, $P_a(R) = P_0$) closer to the receiver ($R << R_{\max}$), the power grows much faster when ν is larger (see (5)), so that closely-located transmitters produce much more interference when ν is large, which, combined with the uniform spatial density of the transmitters, explains the observed behavior. The effect of *m* can be explained in a similar way (i.e. in lower dimensions the transmitters are located, on average, closer to the receiver – see (30)) .

To validate the accuracy of approximations in (33)-(35), and also the expressions for the dynamic range PDF and CDF in the previous section, extensive Monte-Carlo (MC) simulations have been undertaken. Fig. 4–5 show some of the representative results. Note good agreement between the analytical results (including the approximations) and the MC simulations. It can be also observed that the tails of the distributions decay much slower for the $\nu = 4$ case, which indicates higher probability of high-power interference in that case and, consequently, requires higher spurious-free dynamic range of the receiver, in complete agreement with the predictions of the analysis. For example, if $\mathrm{P}_{out} = 10^{-3}$ (i.e. design specification), then, from Fig. 5, the required spurious-free dynamic range of the receiver is $D \approx 50dB$ and $D \approx 90dB$ for the $\nu = 2$ and $\nu = 4$ cases, respectively. Comparing Fig. 5 to Fig. 3, one concludes that higher spurious-free dynamic range is required to sustain the same outage probability when a number of transmitters are present, compared to the case of a single randomly-located transmitter (the difference is 20 dB and 30 dB for the $\nu = 2$ and $\nu = 4$ cases, respectively). Alternatively, a number of interfering transmitters results in higher outage probability compared to the single transmitter case, which is in complete agreement with (34) and is also consistent with intuition.

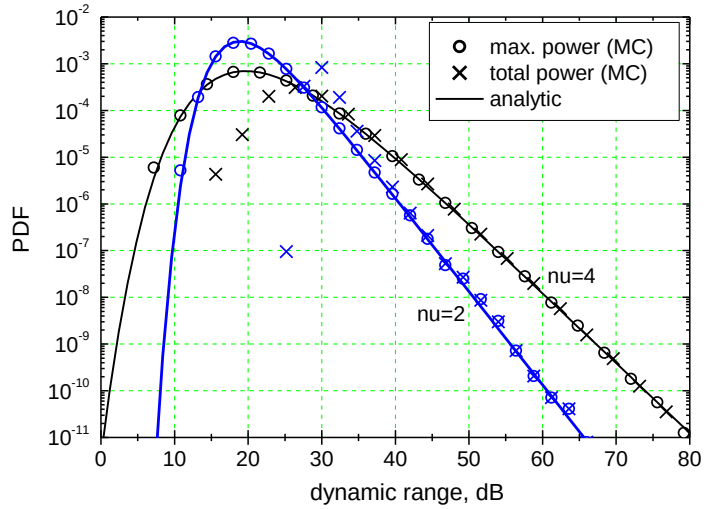

Fig. 4. The PDF of $d_a=P_{a1}/P_0$ and $d_{tot}=P_{tot}/P_0$ evaluated from Monte-Carlo (MC) simulations (10^5 trials) for m=2, ν=2&4, $P_0=10^{-10}$, P_t=1, $\rho=10^{-5}$ and analytic PDF of d_a (see (26))

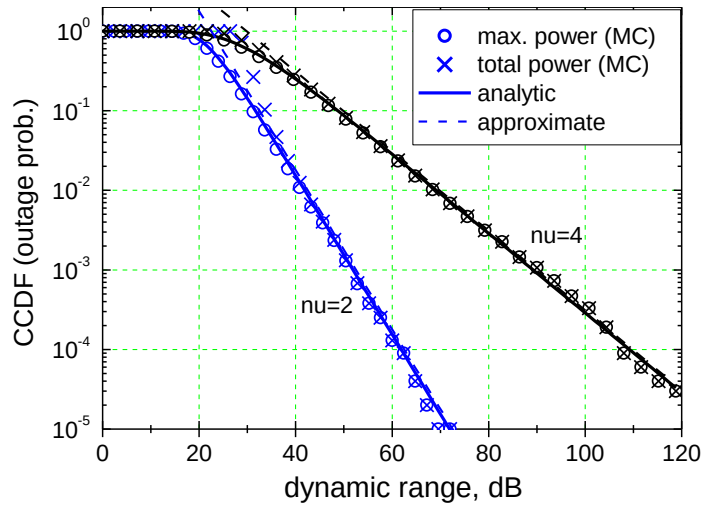

Fig. 5. The CCDF of $d_a=P_{a1}/P_0$ and $d_{tot}=P_{tot}/P_0$ (i.e. the outage probability) evaluated from Monte-Carlo (MC) simulations (10^5 trials) for m=2, ν=2&4, $P_0=10^{-10}$, P_t=1, $\rho=10^{-5}$; analytic CCDF of d_a (derived from (26)) and its approximation in (34) are also shown

Consider now a scenario where the actual outage probability has not to exceed a given value P_{out} for the receiver with a given distortion-free dynamic range D. Using (26) and (31), the average number of transmitters in the active interference zone (ball of radius $r(D)$) can be upper bounded as $\bar{N} \le -\ln(1-\mathrm{P}_{out})$. Using the expression for $\bar{N}$, one obtains a basic tradeoff relationship between the network density and the outage probability,

$$\bar{N} = \int_{V\ r(D)} \rho dV \le -\ln(1-\mathrm{P}_{out}) \qquad (36)$$

i.e. for given outage probability, the network density is upper bounded or, equivalently, for given network density, the outage probability is lower bounded.

In the case of uniform density $\rho = const$ and small outage probability, $\mathrm{P}_{out} << 1$, this gives an explicit tradeoff relationship between the maximum distortion-free interference power at the receiver $P_{\max}$, the transmitter power P_t and the average transmitter density for distortion-free receiver operation,

$$\rho \le c_m^{-1} \mathrm{P}_{out}\ \ P_{\max} / P_t a_\nu \ ^{m/\nu} \qquad (37)$$

or, equivalently, an upper bound on the average density of transmitters in the network.

As intuitively expected, higher $\mathrm{P}_{out}, P_{\max}, \nu$ and lower P_t, m allow for higher network density. The effect of ν is intuitively explained by the fact that higher ν results in larger path loss or, equivalently, in smaller distance at the same path loss, so that the transmitters can be located more densely without increasing interference level. The effect of the other parameters can be explained in a similar way.

B. Ошибка! Объект не может быть создан из кодов полей редактирования. **strongest interfering signals are inactive**

We now assume that $(k-1)$ strongest interfering signals are eliminated via some means (e.g. by filtering or resource allocation). In this case, (28), (29) apply and (33)-(35) generalize to

$$\mathrm{P}_{out} \approx \tfrac{1}{k!}\overline{N}^{k} = \tfrac{1}{k!}\ \overline{N}_{\max} D^{-m/\nu}\ ^{k} \tag{38}$$

$$D \approx\ \overline{N}_{\max} /\!\!/\ k!\mathrm{P}_{out}\ ^{1/k}\ ^{\nu/m} \tag{39}$$

Contrary to the $k=1$ case, P_{out} here is super-linear in $\overline{N}_{\max}$: doubling $\overline{N}_{\max}$ increases P_{out} by the factor $2^k > 2$, i.e. P_{out} is more sensitive to $\overline{N}_{\max}$. Comparing (38), (39) to (34), (35) one can clearly see the beneficial effect of removing $(k-1)$ strongest signals on the outage probability or the required distortion-free dynamic range (note that $\overline{N} << 1$ and $k!\mathrm{P}_{out}\ ^{1/k} >> \mathrm{P}_{out}$ when $\mathrm{P}_{out} << 1$, for $k \geq 2$). Fig. 6 validates this result via MC simulations for $k=2$ (the strongest interferer is eliminated). As an example, at $\mathrm{P}_{out} = 10^{-3}$, the required distortion-free dynamic range is $D \approx 35dB$ and $D \approx 55dB$ for the $\nu = 2$ and $\nu = 4$ cases, respectively, which are significantly smaller than those of the $k=1$ case.

When the actual outage probability has not to exceed the value P_{out}, the average number of transmitters in the active interference zone (the ball of radius $r(D_{df})$) is upper bounded from the following,

$$1 - e^{-\bar{N}} \sum_{i=0}^{k-1} \frac{\bar{N}^i}{i!} \leq \mathrm{P}_{out} \tag{40}$$

which together with $\bar{N} = \int_{V\ r(D)} \rho dV$ constitutes the outage probability-network density tradeoff[6]. Unfortunately, due to the transcendental nature of (40), no closed-form bound on $\bar{N}$ can be obtained in the general case. However, for small outage probability region $\mathrm{P}_{out} << 1 \rightarrow \overline{N} << 1$ and (40) simplifies to,

$$\bar{N} = \int_{V\ r(D)} \rho dV \leq\ k!\mathrm{P}_{out}\ ^{1/k} \tag{41}$$

Comparing (41) to (36), one can clearly see the beneficial effect of "removing" $(k-1)$ most powerful interferers on the outage probability-network density tradeoff, as $k!\mathrm{P}_{out}\ ^{1/k} >> \mathrm{P}_{out}$ in the small outage regime.

In the case of uniform density, (41) reduces to

$$\rho \leq c_m^{-1}\ \ k!\mathrm{P}_{out}\ ^{1/k}\ \ P_{\max} / P_t a_\nu\ ^{m/\nu} \tag{42}$$

---

[6] Note that $(1 - e^{-\bar{N}} \sum_{i=0}^{k-1} \bar{N}^i / i!)$ is a monotonically increasing function of $\bar{N}$ so that the tradeoff point in (40) is unique, and higher P_{out} results in higher admissible $\bar{N}$.

which is a generalization of (37) to $k \geq 1$.

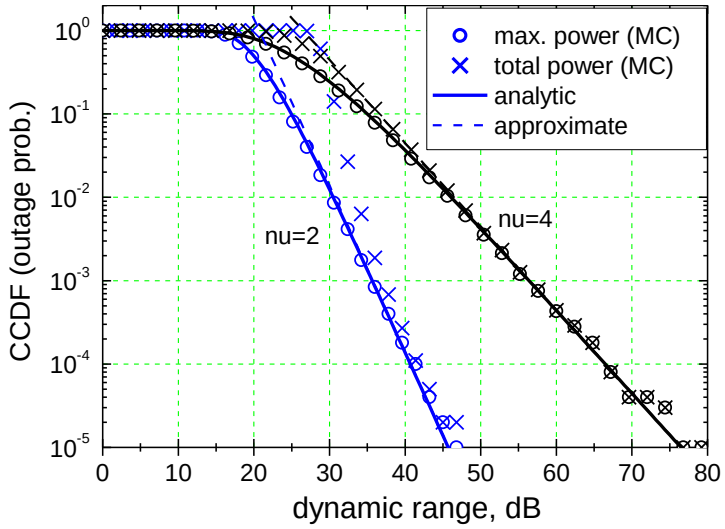

Fig. 6. The CCDF of $d_a=P_{a1}/P_0$ and $d_{tot}=P_{tot}/P_0$ with the most powerful signal cancelled (k=2), evaluated from MC simulations (10^5 trials) and from the analysis, for m=2, ν=2&4, $P_0=10^{-10}$, P_t=1, $\rho=10^{-5}$. Significant improvement over the k=1 case is clear

C. Maximum vs. total interference power

In our analysis, we employed the maximum interference power (or, equivalently, the dynamic range) to define an outage event. It may be argued that the total interference power is a more relevant performance measure, which is extensively used in the current literature (e.g. [1, 2, 11, 13]). In this section, we will show that the total interference power (coming from all interfering transmitter) is dominated by the maximum one (i.e. coming from the closest interfering transmitter) at the region of small outage probability.

As above, consider a network consisting on average of $\overline{N}_{\max}$ interfering transmitters, with each transmitter contributing on average the power $\overline{P_a}$ at the receiver. By the law of large numbers, the total power P_{tot} (coming from all transmitters) is about $P_{tot} \approx \overline{P}_{tot} = \overline{N}_{\max} \overline{P}_a$, i.e. is close to the total power coming from "average" transmitters, which gets more accurate as $\overline{N}_{\max}$ increases, but there is always non-zero probability that P_{tot} exceeds $\overline{P}_{tot}$. If this is the case, one of the possible reasons is that there is a dominant transmitter that contributes more than the average transmitters. For given outage probability P_{out}, the power P_{a1} of the dominant transmitter can be estimated from (35), $P_{a1} = P_0 d_a \geq P_0 D \approx P_0 \left(\overline{N}_{\max} / \mathrm{P}_{out} \right)^{\nu/m}$. This transmitter will provide dominant contribution to P_{tot} if $P_0 D \geq \overline{P_{tot}}$, which can be expressed, using (18), as

$$\mathrm{P}_{out} \leq \begin{cases} \dfrac{\left(\nu/m - 1\right)^{m/\nu} \overline{N}_{\max}^{1-m/\nu}}{D_1^{1-m/\nu}}, & m < \nu \\ 1/\ln D_1, & m = \nu \\ \dfrac{\left(1 - \nu/m\right)^{m/\nu}}{\overline{N}_{\max}^{m/\nu - 1}}, & m > \nu \end{cases} \qquad (43)$$

Clearly, when the outage probability is below a certain threshold, the total power is dominated by the maximum one (i.e. coming from the closest transmitter), so that P_{a1} serves as a good estimate of P_{tot} in the small outage region given by (43). Fig. 5-6 compare the CCDF of P_{a1} and P_{tot} (i.e. the

outage probability) evaluated by Monte-Carlo simulations. Both are quite close in the small outage region, especially for the $m=2,\nu=4$ case. This conclusion is also in agreement with the corresponding observation in [24]. It also suggests an optimum form of interference control: a significant advantage can be gained by eliminating only the single most powerful interferer (compare Fig. 5 to Fig. 6).

Thus, our analysis above also applies when the performance metric depends on the total rather than maximum interference power, in the small outage region.

VI. The Impact of Linear Filtering

In the previous sections, we considered the interfering signals at the Rx input assuming that the Rx antenna was isotropic, i.e. no measures to eliminate some of the interfering signals e.g by linear filtering at the Rx antenna, its frequency filters etc. were considered. In this section, we explore the effect of linear filtering, which may include filtering by the Rx antenna based on the angle of arrival, polarization and frequency, and by linear frequency filters at the receiver (at RF, IF and possibly basedband). Since, as it follows from the previous section, the average number of interfering signals $\overline{N}$ is a key parameter, which determines the dynamic range of interfering signals (see (24),(28)) and ultimately the network density-outage probability tradeoff (e.g. (36), (40)), we consider the impact of linear filtering on this parameter.

Let $\mathbf{z}=[z_1,z_2...z_l]^T$ be the set of filtering variables (i.e. frequency, polarization, angle of arrival etc.) and $f_z(\mathbf{z})$ be the PDF of incoming signals over these variables. The probability of a randomly-chosen input signal falling in the interval $d\mathbf{z}$ is $f_z(\mathbf{z})d\mathbf{z}$, and the probability that the filter output power of this signal exceeds the threshold P_0 is

$$\Pr\ P_{a,out}>P_0\ =\int\limits_{P_0/K(\mathbf{z})}^{\infty} w_a(P)dP=K^{m/\nu}(\mathbf{z}) \tag{44}$$

where $0\le K(\mathbf{z})\le 1$ is the normalized filter power gain, and (15) is used for the PDF $w_a(P)$. Note that $K^{m/\nu}$ represents the reduction in probability of signal power exceeding the threshold from the input (where it is equal to one) to the output of the filter and thus is a filter gain for given filtering variables. The average number of output signals exceeding the threshold in the interval $d\mathbf{z}$ is $d\bar{N}_{out}=K^{m/\nu}(\mathbf{z})f_z(\mathbf{z})d\mathbf{z}d\bar{N}_{in}$, where $d\bar{N}_{in}$ is the average number of input signals exceeding the threshold in the same interval. Finally, the total average number of output signals exceeding the threshold P_0 is

$$\bar{N}_{out}=\bar{N}_{in}/Q,\ Q=\left(\int\limits_{\Delta\mathbf{z}}K^{m/\nu}(\mathbf{z})f_z(\mathbf{z})d\mathbf{z}\right)^{-1}\ge 1 \tag{45}$$

where $\bar{N}_{in}$ is the average number of input signals, Q is the average statistical filter gain, which represents its ability to reduce the average number of visible (i.e. exceeding the threshold) interfering signals, and $\Delta\mathbf{z}$ is the range of filtering variables. This gain further transforms into reduction in the interfering signals' dynamic range (see (24), (28)) or in the outage probability,

$$\mathrm{P}_{out}=1-F_{d,out}(D)=1-e^{-\bar{N}_{out}}\sum_{i=0}^{k-1}\frac{\bar{N}_{out}^{i}}{i!}\approx\frac{\bar{N}_{out}^{k}}{k!}=\frac{1}{k!}\left(\frac{\bar{N}_{in}}{Q}\right)^{k} \tag{46}$$

and also improves the network density-outage probability tradeoff (i.e. (41), (42)),

$$\overline{N_{in}}=\int_{V\ r(D)}\rho dV\le Q\ \ k!\mathrm{P}_{out}\ ^{1/k} \tag{47}$$

$$\rho\le Qc_m^{-1}\ \ k!\mathrm{P}_{out}\ ^{1/k}\ \ P_{\max}/P_t a_\nu\ ^{m/\nu} \tag{48}$$

i.e. the network density ρ can be increased by a factor of Q at the same performance compared to the case of no filtering. Clearly, using directional antennas with highly-directive pattern, for example, results in large Q (similarly to the antenna's gain) and thus the network density can be increased by a large factor Q, as expected intuitively.

VII. Conclusion

In this paper, we introduced a statistical physical-layer model of interference in wireless networks based on standard propagation channel models and a model of random distribution of nodes over a large area of the whole network, which results in a new type of fading, which we termed "network-scale fading" and which is complimentary to the large-scale (shadowing) and small-scale (multipath) fading and is independent of them. The network-scale fading affects the "average" path loss, which becomes a random variable on the network scale. The probability density function of the average power has been derived and used to obtain the distribution of dynamic range of interfering signals and of the outage probability. This analysis culminated in formulation of network density/outage probability tradeoff, which is a result of the interplay between random distribution of the nodes in the network, the propagation path loss and the interference effects at the receiver. The impact of linear filtering (e.g. by the antenna directional pattern) at the received has also been characterized via the average statistical filter gain Q: it allows increasing the network density by a factor of Q at the same outage probability. Possible applications of these results can be in cellular, WiFi/WiMAX and sensor networks. Following the standard approach to the analysis of interference effects on the link performance [10, 11, 13], the combined effect of small-scale, large-scale and network-scale fading is of interest to analyze.

Acknowledgement

The authors would like to thank S. Primak for insightful discussions.

References

1. *Tonguz O.K., Ferrari G.* // Ad Hoc Wireless Networks: A Communication-Theoretic Perspective, Wiley, Chichester, 2006.
2. *Gupta P., Kumar P.R.* // IEEE Trans. Information Theory, Vol. 46, N. 2, P. 388–404, Mar. 2000.
3. *Xie L.L., Kumar P.R.* // IEEE Trans. Information Theory, Vol. 50, N. 5, P. 748–767, May 2004.
4. *Kulkarni S.R., Viswanath P.* // IEEE Trans. Information Theory, Vol. 50, N. 6, P. 1041–1049, Jun. 2004.
5. *Leveque O., Telatar I.E.* // IEEE Trans. Information Theory, Vol. 51, N. 3, P. 858–865, Mar. 2005.
6. *Ozgur A., Leveque O., Tse D.* // IEEE International Symposium on Information Theory (ISIT 2007), Nice, France, June 2007.
7. *Morgenshtern V.I., Bolcskei H.* // IEEE Trans. Information Theory, Oct. 2007.
8. *Boyer J., Falconer D.D., Yanikomeroglu H.* // IEEE Trans. Communications, Vol. 52, N. 10, P. 1820–1830, Oct. 2004.
9. *Boyer J., Falconer D.D., Yanikomeroglu H.* // IEEE Trans. Wireless Communications, Vol. 6, N. 5, P. 1–9, May 2007.
10. *Rappaport T.S.* Wireless Communications: Principles and Practice, Prentice Hall, Upper Saddle River, 2002.
11. *Stuber G.L.* Principles of Mobile Communication (2nd Ed.), Kluwer, Boston, 2001.
12. *Pozar D.M.* Microwave and RF Design of Wireless Systems, Wiley, New York, 2001.
13. *Abu-Dayya A.A., Beaulieu N.C.* // IEEE Trans. Vehicular Technology, Vol. 43, N. 1, P. 164–173, Feb. 1994.
14. *Chiani M., Win M.Z., Zanella A.* // IEEE Trans. Comm., Vol. 51, No. 11, P. 1949–1957, Nov. 2003.
15. *Kwak J.S., Lee J.H.* // IEEE Trans. Vehicular Technology, Vol. 55, No. 1, P. 158–166, Jan. 2006
16. *Gagnon F. et al.* // IEEE JSAC, Vol. 15, N. 4, P. 685–693, May 1997.
17. *Pugachev V.S.* Probability Theory and Mathematical Statistics, Nauka, Moscow, 1979.
18. *Feller W.* An Introduction to Probability Theory and Its Applications, Wiley, 1970.
19. *Mordachev V.I.* Statistical Characteristics of Electromagnetic Environments in Spatially-Scattered Groups of Radio Systems, Technical Report 02880034534, Minsk Radio Engineering Institute, Minsk, USSR, 1987. (in Russian).
20. *Mordachev V.I.* // Proc. of the 9-th Wroclaw Symp. on EMC, June 1988, P. 571–576. (in Russian).
20. *Mordachev V.I.* // Proc. of the 10th Wroclaw Symp. on EMC, June 1990, P. 409–414. (in Russian).
21. *Mordachev V.* Mathematical Models for Radiosignals Dynamic Range Prediction in Space-Scattered Mobile Radiocommunication Networks // The IEEE VTC Fall, Boston, Sept. 24–28, 2000.
22. *Aporovich A.F.* Statistical Theory of Electromagnetic Compatibility of Radio-Electronic Systems, Nauka i Technika, Minsk, 1984. (in Russian).
23. *Tonguz O.K., Ferrari G.* // 3rd IEEE Conf. on Sensor and Ad Hoc Communications and Networks (SECON 06), Vol. 2, P. 715–722, Sept. 2006.